ORIGINAL ARTICLE

Electrospun PAN-Based Carbon Nanofibers for Aqueous Boron Recovery

Ji Wan Park[1] · Su Young Kim[1] · Tae Uk Jeong[1] · Do Young Han[1] · Da Eun Kim[1] · Seong Huh[2] · Yong Sun Won[1]

Abstract

Designed for the recovery of aqueous boron, a critical element with various industrial applications, the use of carbon fibers as an effective adsorbent for boron in aqueous solutions was explored, and the changes in carbon fibers were investigated during repeated boron adsorption and desorption. In this research, prepared PAN fibers by electrospinning were carbonized into nitrogen-doped carbon fibers. The resulting fiber mats undergo boron adsorption in boric acid solution and subsequent regeneration in HCl solution, and these processes repeat multiple times to assess the reusability of carbon fibers. SEM analysis confirmed the successful electrospinning of PAN fibers and their carbonized ones, while EDS and XPS analyses determined the presence of doped nitrogen on the graphene-like surface and the consequential effective boron adsorption. Then ICP-OES showed that the boron adsorption was completed within ~ 1 h to an equilibrium capacity even at room temperature, and the capacity increased with the regeneration of fibers, also confirmed by SEM and BET analyses in that the specific surface area increased along with the physical breakage and shattering of fibers during regeneration. In conclusion, the carbon fibers proposed in this study are applicable for aqueous boron recovery with their operative reusability.

Keywords Carbon nanofiber · Aqueous boron · PAN (polyacrylonitrile) · Electrospinning · Nitrogen-doped

Introduction

Boron (B, atomic number 5) is an essential natural resource (in particular, included in 56 types of rare metals in South Korea), used for various purposes such as glass, special alloys, industrial catalysts, magnetic materials, semiconductor materials, and explosives. Currently, South Korea is entirely dependent on imports for boron. Since a significant increase in imports in 2010, the amount of boron imported has remained stable at around 60,000 tons per year (63,000 tons in 2012, 62,000 tons in 2017), and the import value has also stabilized at a certain level ($103.81 million in 2012, $64.27 million in 2017) [1]. However, Türkiye holds about 70% of the world's boron reserves, and supply problems are more likely due to the Middle East's political instability and the unexpected resource militarization. Considering the world's boron reserves and current production trends, there are concerns about land-based boron as a declining resource and rising prices after about 50 years. On the other hand, although boron in seawater is about 4.5 ppm, the amount of boron dissolved in seawater is about 5.4 trillion tons when considering the capacity of seawater as a whole. If a process to effectively recover boron from seawater develops, it could provide a stable supply to the domestic industrial market and contribute significantly to improving national competitiveness [2]. Research on dissolved boron in seawater has focused on removal rather than recovery. Behind this, seawater desalination using seawater reverse osmosis (SWRO) applies widely, and the boron concentration in drinking water designated by the World Health Organization (WHO) must meet. It is not easy effectively to remove boron using SWRO. Therefore, it is used by the fact that boron in seawater exists in the form of boric acid $(B(OH)_3)$ in neutral conditions and as borate $(B(OH)_4^-)$ of increased molecular size as pH increases. By configuring a two-pass SWRO process and bypassing a part of the process water

✉ Seong Huh
  shuh@hufs.ac.kr

✉ Yong Sun Won
  yswon@pknu.ac.kr

1 Department of Chemical Engineering, Pukyong National University, Busan 48513, Republic of Korea

2 Department of Chemistry and Protein Research Center for Bio-Industry, Hankuk University of Foreign Studies, Yongin 17035, Republic of Korea

while increasing the pH, the borate is removed from the negatively charged SWRO membrane, thus controlling the boron concentration in the final drinking water [3]. However, in 2011, the WHO revised the boron concentration in drinking water from 0.5 to 2.4 ppm, making it possible to remove boron using a two-pass SWRO system readily [4].

In this regard, polyols such as xylitol and mannitol with multiple hydroxyls form large complexes when reacted with boron species, and these complexes are removed efficiently through reverse osmosis membranes [5, 6]. Later, a membrane-type polyvinyl alcohol (PAV) mat directly integrated with existing RO membranes was developed to address the potential issue of fouling and additional burden on the RO membrane due to polyols [7]. A PVA mat with multiple hydroxyl ligands was electrospun and stabilized in methanol, and it could chemically adsorb boron in a neutral aqueous solution without structural collapse [8]. However, when using the PVA mats for boron recovery, one needs acidic strong conditions to desorb the chemisorbed boron from the PVA matrix, and acidic solutions completely dissolved the PVA mat [7]. Therefore, exploring new materials with multiple hydroxyl ligands that possess structural stability even under acidic conditions for aqueous boron recovery through the typical adsorption–desorption cycles was necessary.

Meanwhile, a recent study reported using nitrogen-doped graphene oxide for the adsorption of boron in seawater [9]. Inspired by this research, we proposed nitrogen-doped carbon fibers for aqueous boron recovery that can be easily prepared by electrospinning polyacrylonitrile (PAN) fibers and carbonizing them in an inert atmosphere to induce nitrogen doping on the surface of the carbon fibers [10, 11]. A theoretical study using the density functional theory (DFT) molecular modeling showed that the nitrogen-doped graphene surface is capable of boron adsorption from aqueous boric acid via dehydration reactions having viable activation energies. More specifically, adjacent carbons to the doped nitrogen are hydrated with multiple hydroxyl ligands, and these hydroxyl groups react with boric acid to be chemisorbed on the surface, as illustrated in a schematic in Fig. 1 [12, 13]. In addition, X-ray photoelectron spectroscopy

(XPS) confirmed the creation of a nitrogen-doped graphene-like surface and its ability to adsorb aqueous boron on the surface [9].

We now present a comprehensive study evaluating the stability of nitrogen-doped carbon fibers for aqueous boron recovery. First, deconvolution of the various elemental XPS peaks is performed to compare the chemical states of elements on the fiber surface before and after adsorption. Second, an inductively coupled plasma optical emission spectrometer (ICP-OES) quantitatively determines the fiber's equilibrium adsorption capacity by measuring the amount of boron in aqueous solution before and after adsorption. Third, we evaluate our presumption with that the carbon fibers maintain their structural stability under acidic conditions and are reusable in repeated adsorption–desorption processes (typically required in the aqueous boron recovery) by monitoring the adsorption capacity, surface morphology, and the surface area of the fibers throughout multiple adsorption–desorption stages. It employs ICP-OES, scanning electron microscopy (SEM), and Brunauer–Emmett–Teller (BET) analysis, respectively.

Experimental

Preparation of Nitrogen-Doped Carbon Fibers

PAN fibers were easily prepared from a magnetically well-stirred PAN and dimethylformamide (DMF) by an electrospinning machine (ESP-100D, NanoNC, South Korea) at room temperature. The PAN fibers were then carbonized consecutively in a tubular furnace (SH-FU-1200STG-WG, SH Scientific, South Korea) at 300 °C in air and carbonized at 1000 °C in argon atmosphere, respectively. Argon was purged twice before carbonization to remove remnant oxygen. The resulting carbon fibers are anticipated to generate nitrogen-doped graphene-like surface due to the inherent nitrogen in PAN. The detailed operating conditions were presented in our previous study [13].

Fig. 1 Schematic of the boron adsorption mechanism onto the N-doped graphene surface via two-step dehydration [13]
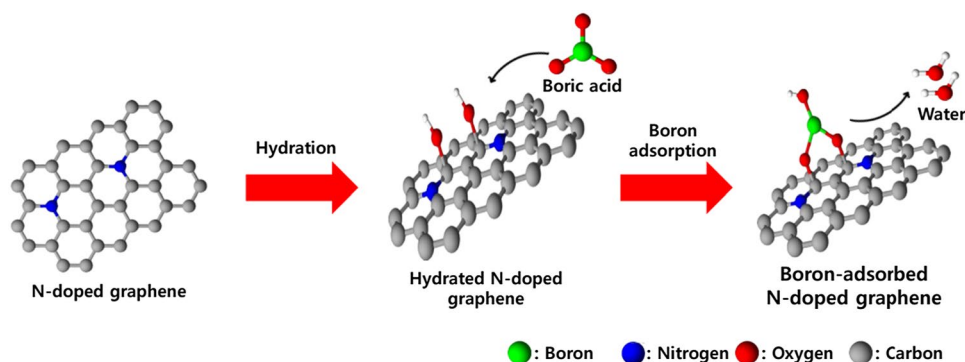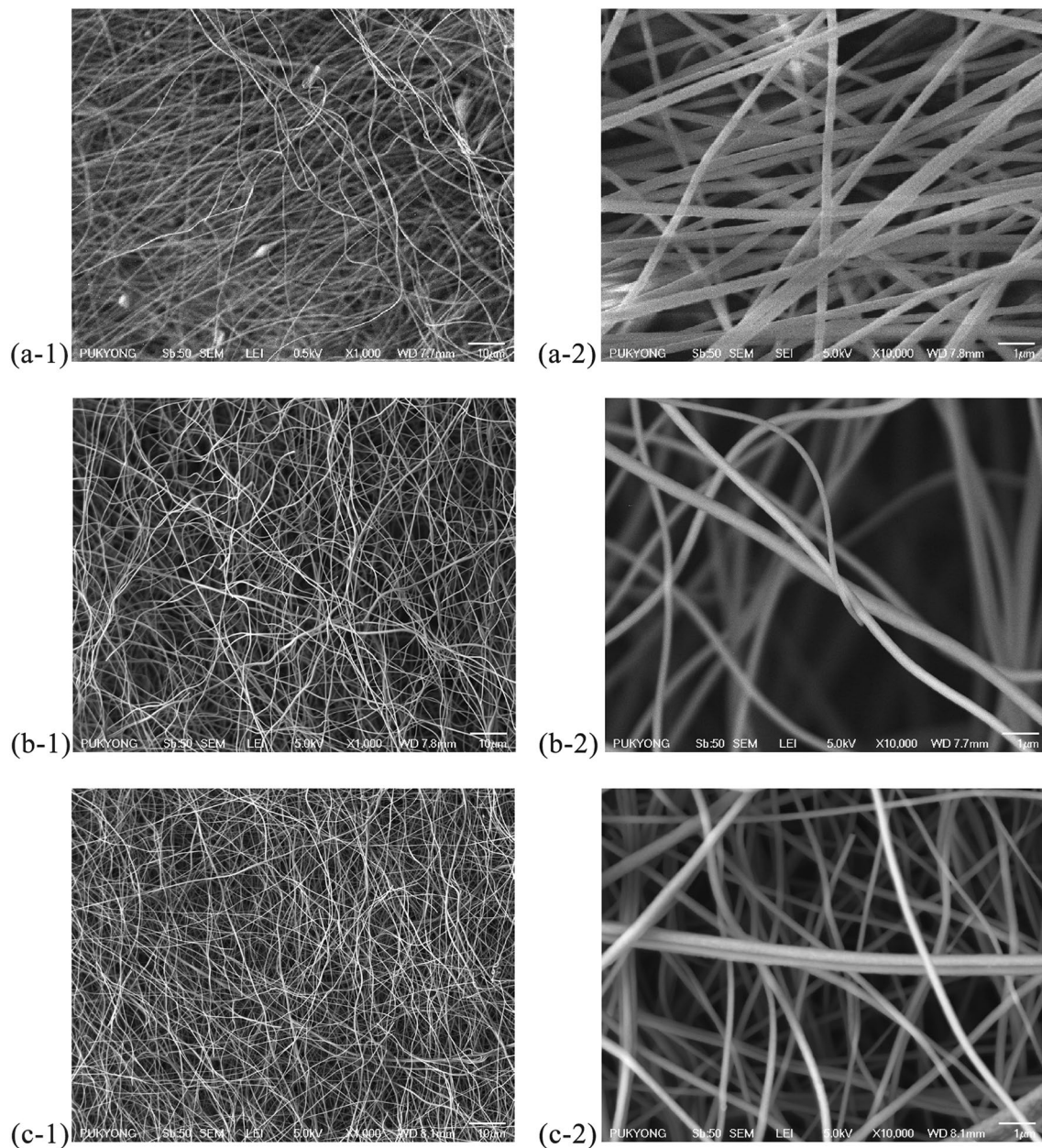
Fig. 2 SEM images of the electrospun PAN fibers (**a**), carbon fibers (**b**), and carbon fibers with aqueous boron adsorbed (**c**) at different magnifications (1; ×1000, 2; ×10,000)

Measurements

To qualitatively confirm the capacity of carbon fibers for aqueous boron adsorption, the sample was immersed in a solution of 0.1 M boric acid for 24 h, and cleansed with distilled water before drying in a vacuum oven at 100 °C for 12 h. Then the chemical states of the carbon fiber surface before and after boron adsorption were analyzed by XPS (AXIS Supra, KRATOS Analytical Ltd.), while the surface morphology and constitution were observed by a SEM

(JSM-7401F, JEOL) and its implemented energy dispersive spectroscopy (EDS).

A quantitative analysis was required to establish the material balance for the adsorption process. Therefore, an ICP-OES (Avio 500, PerkinElmer) was employed to accurately measure the amount of aqueous boron in the boric acid solution before and after adsorption. The change of aqueous boron concentration in solution is assumed to be equivalent to the amount of adsorbed boron on carbon fibers. Solution samples were collected for 30 min to 24 h immersion periods to determine the carbon fiber's equilibrium adsorption
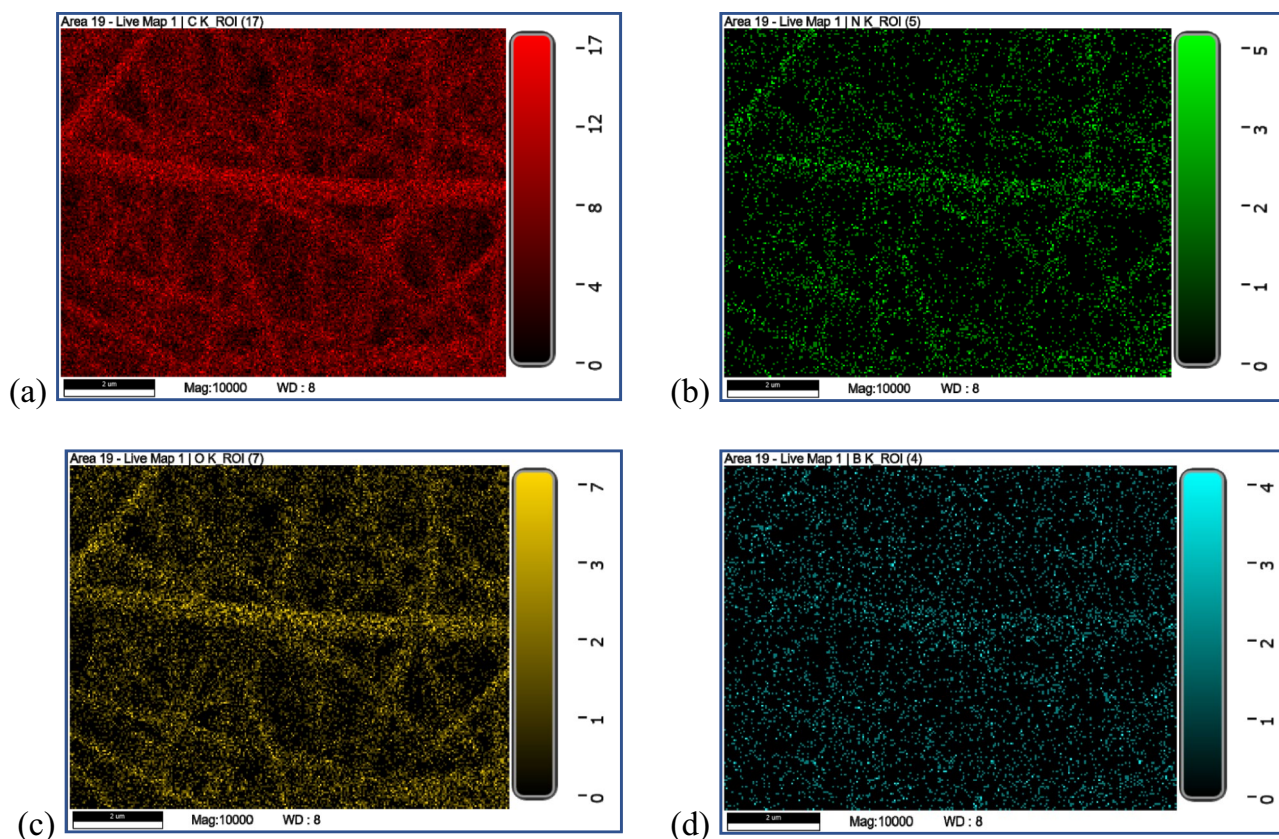
Fig. 3 EDS elemental mapping on the carbon fibers with aqueous boron adsorbed at the magnification of ×10,000; **a** carbon, **b** nitrogen, **c** oxygen, and **d** boron

Table 1 Atomic concentrations measured by EDS

Element	Before the 1st adsorption	After the 1st adsorption	Before the 2nd adsorption (post to regeneration)	After the 2nd adsorption
C	94.3	83.29	95.5	82.94
N	3.7	2.24	3.4	3.02
O	2.1	4.95	1.1	4.81
B	–	9.52	–	9.23

capacity. Then the whole measurement procedure repeats the 2nd adsorption of the sample regenerated in acidic conditions (in other words, with the boron desorbed out of the sample) to check out the change of the equilibrium adsorption capacity. The boron desorption was processed in 0.1 M HCl solution for 24 h, and the sample was cleansed with distilled water before being dried in a vacuum oven at 100 °C for 12 h.

Finally, the structural integrity of the carbon fibers was evaluated until the regeneration of the sample was extended by four times. SEM observed the surface morphology change, and the specific surface change was measured by a gas sorption analyzer (Quantachrome autosorb-iQ, Andon Paar Korea Ltd.).

Results and Discussion

The surface morphology changes of electrospun PAN fibers, the carbon fibers (treated by the stabilization and carbonization), and aqueous boron adsorbed carbon fibers (immersed in the boric acid solution for 24 h) were observed by SEM as shown in Fig. 2. The electrospinning of PAN fibers and stabilization/carbonization were successful. Nanofibers with a diameter of about ~200 nm are identified clearly without much structural difference, even for the fibers soaked in the boric acid solution. Because the atomic constitution measured by EDS could be primitive criteria for the boron adsorption capability of the carbon fibers, Fig. 3 presents the
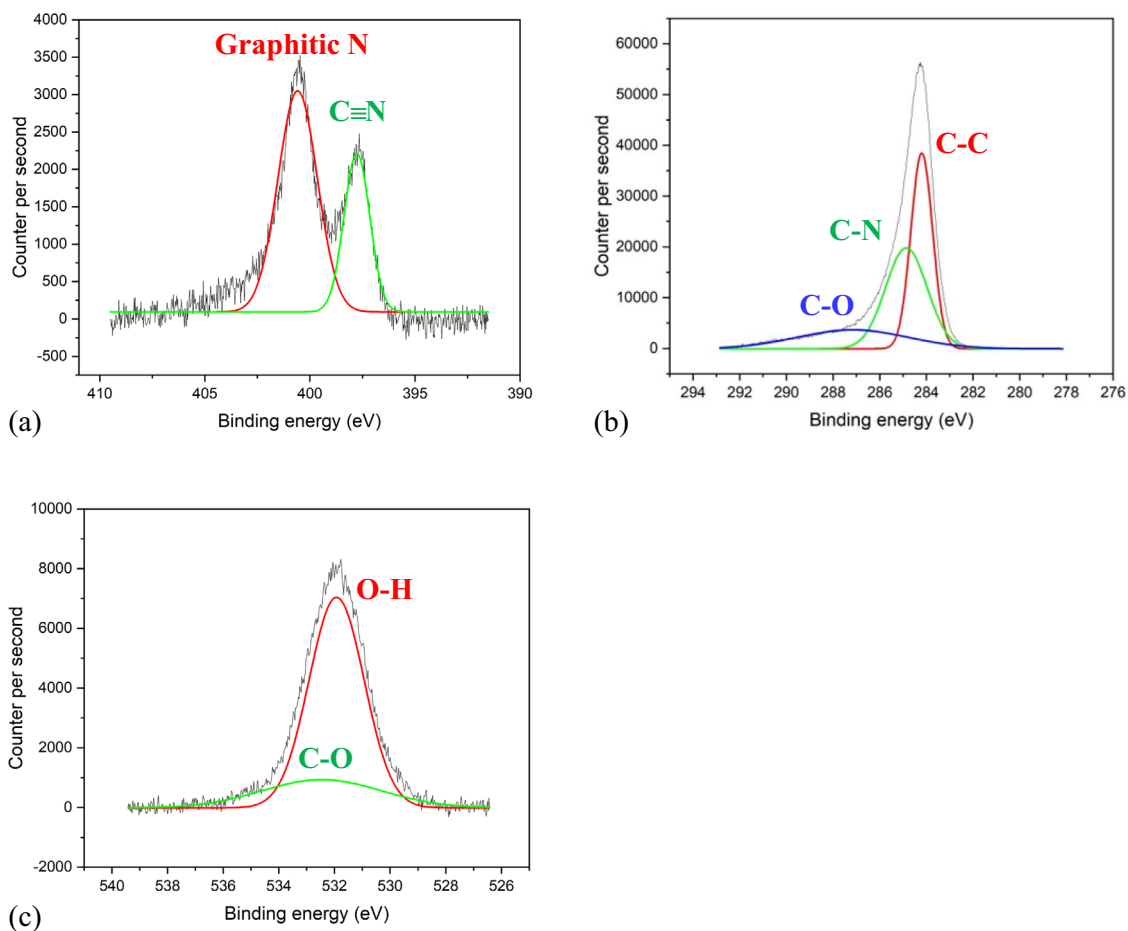
Fig. 4 XPS elemental peak deconvolutions for the carbon fibers before the adsorption: **a** N1s, **b** C1s, and **c** O1s

EDS elemental mapping on the fibers with aqueous boron adsorbed. The nitrogen and boron as well as carbon and oxygen were detected homogeneously in a similar manner along with the fibers. Therefore, it suggests that nitrogen-containing carbon fibers are effectively prepared and capable of adsorbing boron. The atomic concentrations measured by EDS support the proposition too, as shown in Table 1. For the carbon fibers with boron adsorbed, the oxygen content is enhanced because the aqueous boron takes part in the adsorption on the N-doped graphene-like surface in the form of boric acid and thus, the oxygen would stick together [12, 14]. Next, we were to verify that the adsorbed boron was removed entirely during the regeneration in acidic conditions and that the resulting samples are reusable for the 2nd aqueous boron adsorption. At least, it was positive by EDS constitutional analyses (see Table 1).

To finalize whether the boron adsorbs chemically on the nitrogen-doped graphene-like surface, the chemical states of relevant elements were analyzed through XPS peak deconvolutions. The samples were compared before and after adsorption, as shown in Figs. 4 and 5. At first, the graphitic

nitrogen peak at 400.6 eV in Fig. 4a indicates the construction of an N-doped graphene-like surface, and its height is much higher than that of the C≡N peak at 397.8 eV made from PAN which demonstrates a quite decent degree of carbonization [11]. In accordance, dominant C–C bonds of the graphene-like surface at 284.2 eV were detected along with C–N bonds for nitrogen doping at 284.8 eV (see Fig. 4b) [15]. Meanwhile, the C–O peak at 287.2 eV may originate from the dehydration of carbon atoms adjacent to doped-nitrogen atoms on the graphene surface (see Fig. 1). In Fig. 4c, the C–O peak at 443 eV is attributed to the hydration of carbon atoms (see Fig. 1). The significant O–H peak probably comes from physical water molecules on the sample surface. In comparison, the B–O peaks appear at 192.3 and 432 eV with the boron adsorption, as shown in Fig. 5c, d, respectively. In our previous study (see Fig. 1), boric acid reacts with the hydroxyl groups of the carbon atoms adjacent to the doped nitrogen to produce one or two waters by dehydration [10, 11, 13], thus enabling that the chemical state of adsorbed boron would be of B–O bonds. Table 2 shows the atomic concentrations measured by XPS with a
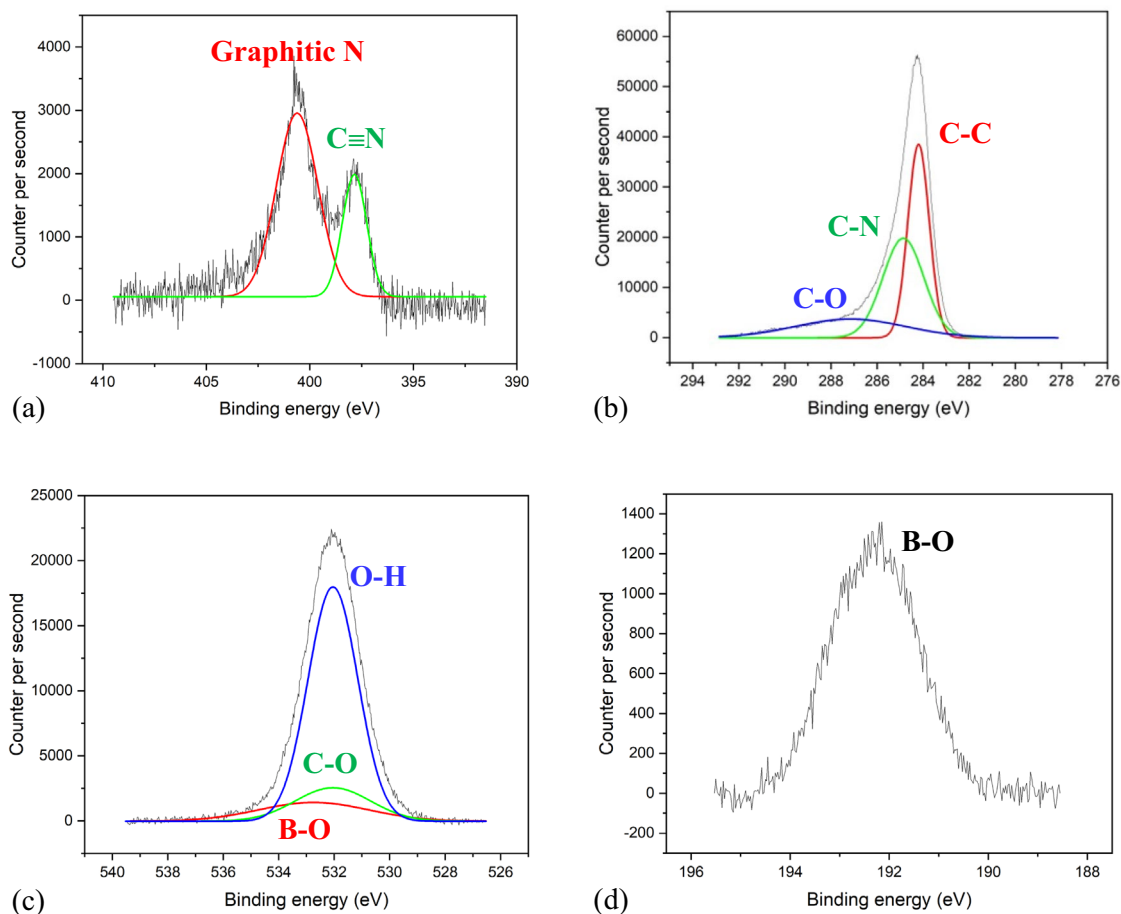
Fig. 5 XPS elemental peak deconvolutions for the carbon fibers after the adsorption: **a** N1s, **b** C1s, **c** O1s, and **d** B1s

Table 2 Atomic concentrations measured by XPS

Element	Before the 1st adsorption	After the 1st adsorption	Before the 2nd adsorption (post to regeneration)	After the 2nd adsorption
C	87.8	79.2	86.9	69.3
N	5.5	3.1	4.5	5.7
O	6.1	14.2	8.0	20.6
B	0.6	3.6	0.6	4.4

similar trend as Table 1. The presence of 0.6 at.% boron in the samples before the 1st adsorption and after the 1st regeneration, shown in the 2nd column and the 4th column in Table 2 respectively, is probably artificial because it was the same even for the case immersed in distilled water.

However, the atomic concentrations obtained by EDS and/or XPS (see Tables 1 and 2) were lacking for determining the carbon fibers' capacity of boron adsorption, just confirming their capability of boron adsorption. An ICP-OES analysis of boron amount in the boric acid solution was used to determine the carbon fibers' adsorption capacity. The decrease in boron concentration in the solution was assumed to be equivalent to the amount of boron adsorbed on the carbon fibers, and solution samples for ICP-OES were collected by the amount of 20 mL at 30 min, 1, 2, 3, 5, 7, 9, 12, and 24 h after the carbon fibers were immersed in the boric acid solution. Table 3 summarizes the boron concentrations in solution measured by ICP-OES and the converted amount of adsorbed boron concerning the adsorption duration. The value of 1061.43 mg/L in the 1st row of Table 3 equals a total of 21.23 mg boron in 20 mL solution

Table 3 Boron concentration in solution measured by ICP-OES and converted amount of adsorbed boron concerning the duration of the adsorption

Adsorption duration (h)	Boron conc. for the 1st adsorption (mg/L)	Boron conc. for the 2nd adsorption (mg/L)[a]	Cumulative adsorbed boron for the 1st adsorption (mg)	Cumulative adsorbed boron for the 2nd adsorption (mg)[a]
0 (reference)	1061.43	966.19	–	–
0.5	992.32	918.83	12.44	8.53
1	951.67	864.10	18.94	17.76
2	982.64	903.10	14.61	11.88
3	984.64	882.2	14.37	14.39
5	913.772	882.5	21.45	14.36
7	858.16	870.36	25.90	15.33
9	878.32	886.15	24.69	14.38
12	888.55	839.48	24.28	16.25
24	890.09	776.05	24.25	17.52

[a]The 2nd adsorption was proceeded with carbon fibers regenerated in 0.1 M HCl solution
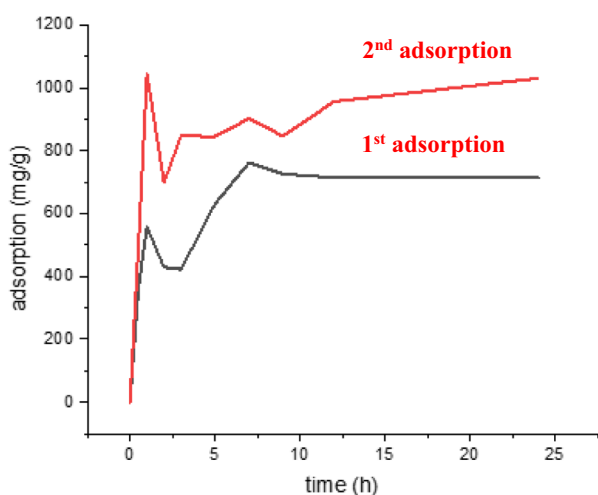

Fig. 6 Boron adsorption capacity (mg/g) of carbon fibers concerning the adsorption duration. The 2nd adsorption proceeded with carbon fibers regenerated in 0.1 M HCl solution

($= 1061.428$ mg/L $\times 20$ mL $\times 10^{-3}$ L/mL). Although the value of 966.192 mg/L for the 2nd adsorption is slightly different, any error depending on instrumental conditions might cancel out through the subtraction and cumulation in the following conversion. The carbon fibers were in a mat form, and we severed them by 3 cm $\times$ 3 cm to be weighed. For a 200 mL beaker of 0.1 M boric acid solution, 20 mL solution was collected for ICP-OES analysis in the 1st place, and the remnant 180 mL solution was ready for the immersion of carbon fibers. Another 20 mL solution was then collected at every given duration (30 min, 1 h, 2 h, and so forth) for subsequent ICP-OES analyses. Table 3 provides the cumulative amount of adsorbed boron calculated from the difference of boron concentrations at every given duration and the solution

volume decrease. Figure 6 shows the adsorption capacity of adsorbed boron amount divided by the weight of carbon fibers (0.034 and 0.017 g for the 1st and 2nd adsorption steps, respectively). The mat happened to break almost half during the regeneration, and thus one was used for the 2nd adsorption. Meanwhile, the boron adsorption is relatively fast enough to be completed within ~ 1 h even under room temperature, which is well-matched with our previous study [13] that dehydration reactions accompanied by the boron adsorption on the nitrogen-doped graphene surface possess viable activation barriers. Nonetheless, the maximum (or equilibrium) adsorption capacity of 700–1000 mg/g is unusually high to be accepted compared to 58.7 mg/g of nitrogen-doped graphene oxide [16]. It must be because of an inappropriate combination of too high a concentration (0.1 M) of boric acid feed solution and too low a weight of adsorption media (carbon fibers or mat). Even the carbon fibers (or mat) of 3 cm $\times$ 3 cm were extraordinarily light, and also the collected solution samples had diluted for ICP-OES analyses. In fact, the values in Table 3 themselves are measured ones multiplied by a dilution factor. However, the trend is supposed to be noteworthy. In that sense, more meticulously designed bench-scale experiments with large carbon fibers and the boron concentration in feed solution close to that of seawater are needed.

Now, we focus on why the boron adsorption capacity increases when carbon fibers are reused, as shown in Fig. 6, and the relevant structural integrity of carbon fibers under multiple regeneration steps. Because we witnessed our sample in half during the regeneration, further investigations on the structural integrity of carbon fibers proceeded. Figure 7 presented the SEM micrographs of carbon fibers when the regeneration extends up to four times—every regeneration (or boron desorption) over in 0.1 HCl solution for 24 h. Not only was structural damage such as shattering detected
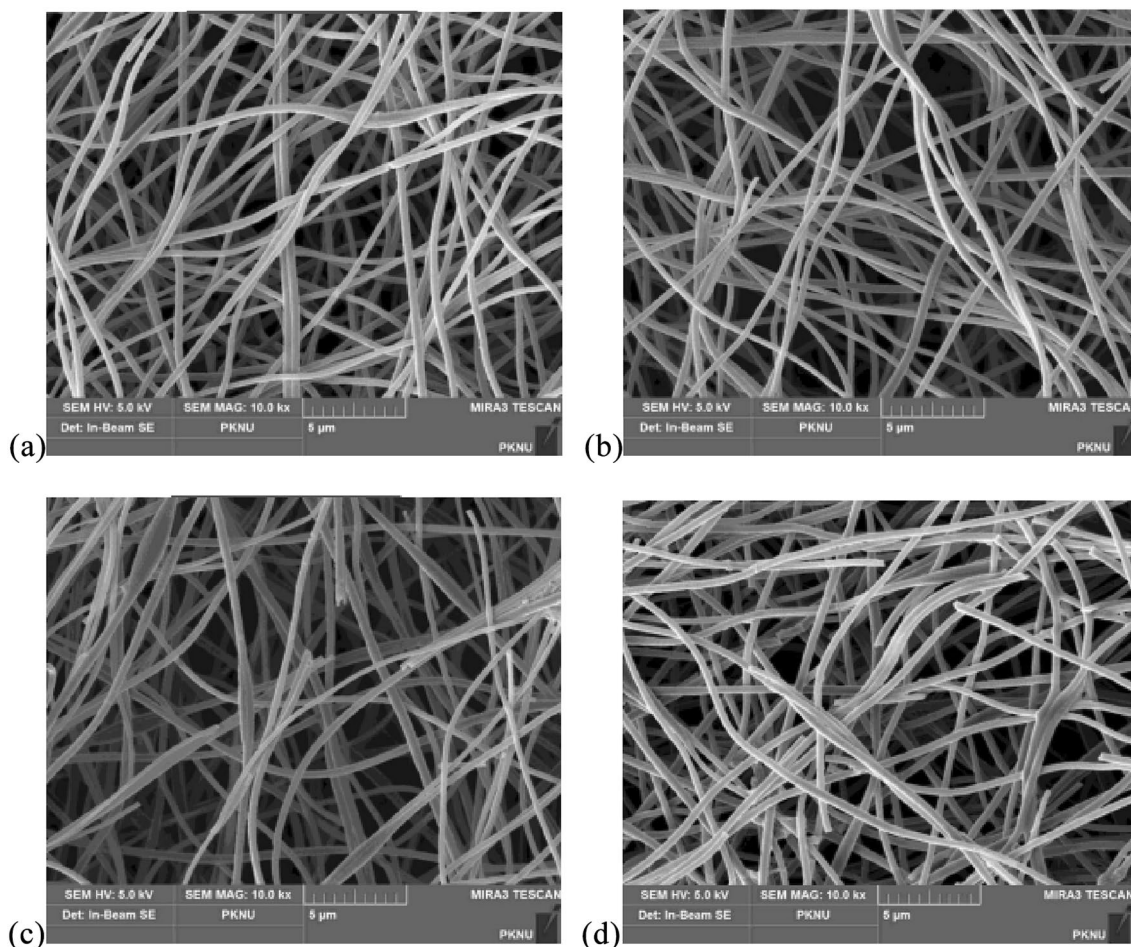
Fig. 7 SEM micrographs of the carbon fibers after the regeneration at acidic conditions at the magnification×10,000; **a** once, **b** twice, **c** three times, and **d** four times
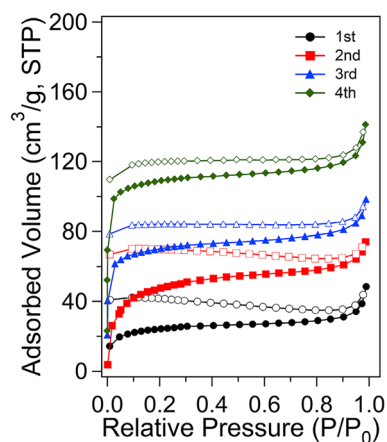

Fig. 8 The N_2 adsorption–desorption isotherms measured at 77 K of carbon fibers regenerated once, twice, thrice, and four times. Open and solid symbols represent adsorption and desorption branches, respectively

visually, but microscopical cutoff of fibers also developed as the regeneration repeats, as shown in Fig. 6. However, the robustness of carbon fibers is reasonably confirmed, considering that the carbon fibers were soaked in acidic conditions for 24 h at every regeneration step. The specific surface area change was also measured by BET analysis, as shown in Fig. 8, increasing 85, 174, 242, and 367 m^2/g sequentially. It suggests that the nitrogen-doped graphene-like surface as a venue of boron adsorption is emerging more by unraveling fiber matrix and physical damage by the effect of regeneration in acidic conditions for an extended period. This surface area increase corresponds to the boron adsorption capacity increase with the regeneration step in Fig. 6. The pore volume and pore size (not shown here) obtained by the Barrett–Joyner–Halenda (BJH) method were 0.075/0.11/0.15/0.22 cm^3/g and 1.51/1.23/0.88/0.95 nm, respectively. These low values mean that carbon fibers in this study are non-porous.

Conclusion

Carbon fibers prepared by the carbonization of electrospun and stabilized PAN fibers should have nitrogen-doped graphene-like surface suitable for aqueous boron adsorption. SEM/EDS measurements showed the presence of nitrogen in the fiber matrix and boron upon the boron adsorption. A further XPS study also confirmed the evidence of graphitic N (nitrogen doping) and B–O bond. The boric acid ($B(OH)_3$) is chemically adsorbed by dehydration with hydroxyl groups of the carbon adjacent to the doped nitrogen, and the possible bond type associated with boron is B–O.

ICP-OES measurements of the boron concentration in the solution with respect to the adsorption duration indirectly determined the fibers' boron adsorption capacity. The results demonstrated that the adsorption occurs relatively fast and completes within ~ 1 h, and the efficiency increases when carbon fibers are reused (or regenerated). Viable activation barriers of the corresponding reactions should promote the boron adsorption even in room temperature. The capacity enhancement is then possibly attributed to the specific area increase of carbon fibers due to structural changes (or surface area increase), like the breakage of fibers and shattering during the regeneration in acidic conditions, confirmed by BET measurements and SEM observations. However, the expected robustness of carbon fibers assures reasonable against for physical (or mechanical) damage.

References

1. Resource Statistics Portal, Korea Institute of Geoscience and Mineral Resources (KIGAM), *Korea Mineral Information* (2017)

2. S. Jung, M.-J. Kim, J. Korean Inst. Resour. Recycl. **25**(4), 3–10 (2016)

3. K.H. Eom, H.C. Jeong, H.Y. An, J.-H. Lim, J.-K. Lee, Y.S. Won, Korean Chem. Eng. Res. **53**(6), 1–6 (2015)

4. World Health Organization (WHO), *Boron in drinking water—background document for development of WHO guidelines for drinking water quality* (2009)

5. M.-K. Kim, K.H. Eom, J.-H. Lim, J.-K. Lee, J.D. Lee, Y.S. Won, Korean J. Chem. Eng. **32**(11), 2330–2334 (2015)

6. B. Park, J. Lee, M. Kim, Y.S. Won, J.-H. Lim, S. Kim, Desalin. Water Treat. **57**(17), 7910–7917 (2016)

7. K.S. Lee, K.H. Eom, J.-H. Lim, H. Ryu, S. Kim, D.-K. Lee, Y.S. Won, J. Phys. Chem. A **121**(11), 2253–2258 (2017)

8. J. Wang, T. Wang, L. Li, P. Wu, K. Pan, B. Cao, J. Water Process. Eng. **3**, 98–104 (2014)

9. F. Chen, L. Guo, X. Zhang, Z.Y. Leong, S. Yang, H.Y. Yang, Nanoscale **9**(1), 326–333 (2017)

10. E. Jo, S. Lee, K.T. Kim, Y.S. Won, H.-S. Kim, E.C. Cho, U. Jeong, Adv. Mater. **21**(9), 968–972 (2009)

11. X.-L. Sun, Z. Liu, Z.-L. Cheng, J. Hazard. Mater. **389**, 121879 (2020)

12. A.S. Rad, A. Shadravan, A.A. Soleymani, N. Motaghedi, Curr. Appl. Phys. **15**(10), 1271–1277 (2015)

13. S.H. Hong, S.-G. Han, S.Y. Kim, Y.S. Won, Clean Technol. **28**(3), 210–217 (2022)

14. Y.T. Wei, Y.M. Zheng, J.P. Chen, Water Res. **45**(6), 2297–2305 (2011)

15. G. Wu, C. Lu, X. Wu, S. Zhang, F. He, L. Ling, J. Appl. Polym. Sci. **94**(4), 1705–1709 (2004)

16. K. Yokwana, B. Ntsendwana, E.N. Nxumalo, S.D. Mhlanga, J. Mater. Res. **38**, 3239–3263 (2023)